Cell, Vol. 90, 121–129, July 11, 1997, Copyright ©1997 by Cell Press

Developmentally Regulated Mitochondrial Fusion Mediated by a Conserved, Novel, Predicted GTPase

Karen G. Hales* and Margaret T. Fuller*†
*Department of Genetics
†Department of Developmental Biology
Stanford University School of Medicine
Stanford, California 94305

Summary

The Drosophila melanogaster *fuzzy onions* (*fzo*) gene encodes the first known protein mediator of mitochondrial fusion. During Drosophila spermatogenesis, mitochondria in early postmeiotic spermatids aggregate, fuse, and elongate beside the growing flagellar axoneme. *fzo* mutant males are defective in this developmentally regulated mitochondrial fusion and are sterile. *fzo* encodes a large, novel, predicted transmembrane GTPase that becomes detectable on spermatid mitochondria late in meiosis II, just prior to fusion, and disappears soon after fusion is complete. Missense mutations that alter conserved residues required for GTP binding in other GTPases inhibit the fusogenic activity of Fzo in vivo but do not affect its localization. Fzo has homologs of unknown function in mammals, nematodes, and yeast.

Introduction

Mitochondria undergo regulated fusion in many cell types (Skulachev, 1990; Kawano et al., 1995). Serial sections from rodent skeletal muscle (Kirkwood et al., 1986), lymphocytes (Rancourt et al., 1975), liver (Brandt et al., 1974), spinal ganglion cells (Hayashida, 1973), and the yeast S. cerevisiae (Stevens, 1981) have revealed that mitochondria within a cell can exist as a giant branched reticulum. Skulachev (1990) proposed that mitochondrial reticula support coordinated and efficient ATP production by allowing widespread transmission of membrane potential to oxygen- or nutrient-poor regions of a cell. Mitochondrial fusion is developmentally regulated in rat diaphragm muscle (Bakeeva et al., 1981), liver (Smith, 1931), Drosophila spermatids (Fuller, 1993), and many single-celled eukaryotes (Kawano et al., 1995). In S. cerevisiae, mitochondria fuse after mating (Dujon, 1981) and during meiosis and sporulation (Stevens, 1981). Mitochondria in Physarum polycephalum fuse during plasmodium formation and sporulation if a linear mitochondrial plasmid is present (Takano et al., 1994). Neither the fusion mediator in P. polycephalum nor any other mitochondrial fusogen has been identified.

Protein mediators of membrane fusion in other contexts are known. Hemagglutinin mediates fusion of endocytosed viruses to cells (Hernandez et al., 1996). In the secretory pathway, docking specificity between vesicles and organelles is provided by integral membrane SNARE proteins on each compartment (Rothman, 1996). Either the ATPase NSF (Rothman, 1996) or a yet unidentified protein (Mayer et al., 1996) could alter SNARE conformation and trigger bilayer fusion. Vesicle trafficking also requires Rab GTPases, which appear to regulate SNARE assembly during vesicle docking (Pfeffer, 1996).

We have investigated molecular requirements for mitochondrial fusion in Drosophila spermatogenesis. Mitochondria undergo dramatic morphogenetic changes during spermatid differentiation in Drosophila (Fuller, 1993). In early postmeiotic spermatids, mitochondria aggregate beside each haploid nucleus and fuse into exactly two giant mitochondrial derivatives that wrap around each other to form the spherical Nebenkern (Figure 1A). The Nebenkern resembles an onion slice when viewed in cross section by transmission electron microscopy (TEM; Figure 1D); hence the term "onion stage" refers to early round spermatids. Serial section analysis confirmed that the onion stage Nebenkern contains two topologically distinct compartments (Tates, 1971). During flagellar elongation, the two mitochondrial derivatives unfurl from each other and elongate beside the growing axoneme (Tates, 1971; Tokuyasu, 1974; Figure 1A).

Here, we describe identification of the *fuzzy onions* (*fzo*) gene, which encodes the first known mediator of mitochondrial fusion. *fzo* mutant males are sterile and have defects in postmeiotic fusion of mitochondria. *fzo* encodes a novel, predicted transmembrane GTPase associated with spermatid mitochondria during the time of fusion. Missense mutations in conserved GTPase motifs eliminated or reduced Fzo function but did not affect its localization. Fzo has homologs in mammals, nematodes, and yeast and is the first member of known function in a novel family of large, predicted, multidomain GTPases.

Results

fzo Is Required for Developmentally Regulated Mitochondrial Fusion

Mutations in *fzo* cause male sterility and defects in mitochondrial fusion during Nebenkern formation. In *fzo* early spermatids, mitochondria aggregate, forming misshapen Nebenkerns as viewed by phase contrast microscopy (Figure 1C, arrowhead), and fail to fuse into two giant mitochondria. Instead, many smaller mitochondria appear to wrap around each other at the onion stage (Figure 1E). Despite the prior defect in fusion, mitochondria unfurl and elongate in *fzo* mutants. Early elongating mitochondria in *fzo* mutants appear fragmented (Figure 1G, arrowhead) compared to wild type (Figure 1F). At later stages, each *fzo* spermatid has many elongating mitochondria (Figures 1I and 1K), rather than the normal two elongating mitochondrial derivatives (Figures 1H and 1J). Thus the defects in *fzo* mutant spermatids appear specific for mitochondrial fusion, as mitochondrial aggregation, membrane wrapping, and elongation all occur. In addition, spermatid mitochondria in *fzo* mutants take up rhodamine 123 as in wild type (not shown), indicating presence of a membrane potential and suggesting that *fzo* mutations probably do not grossly affect respiration.

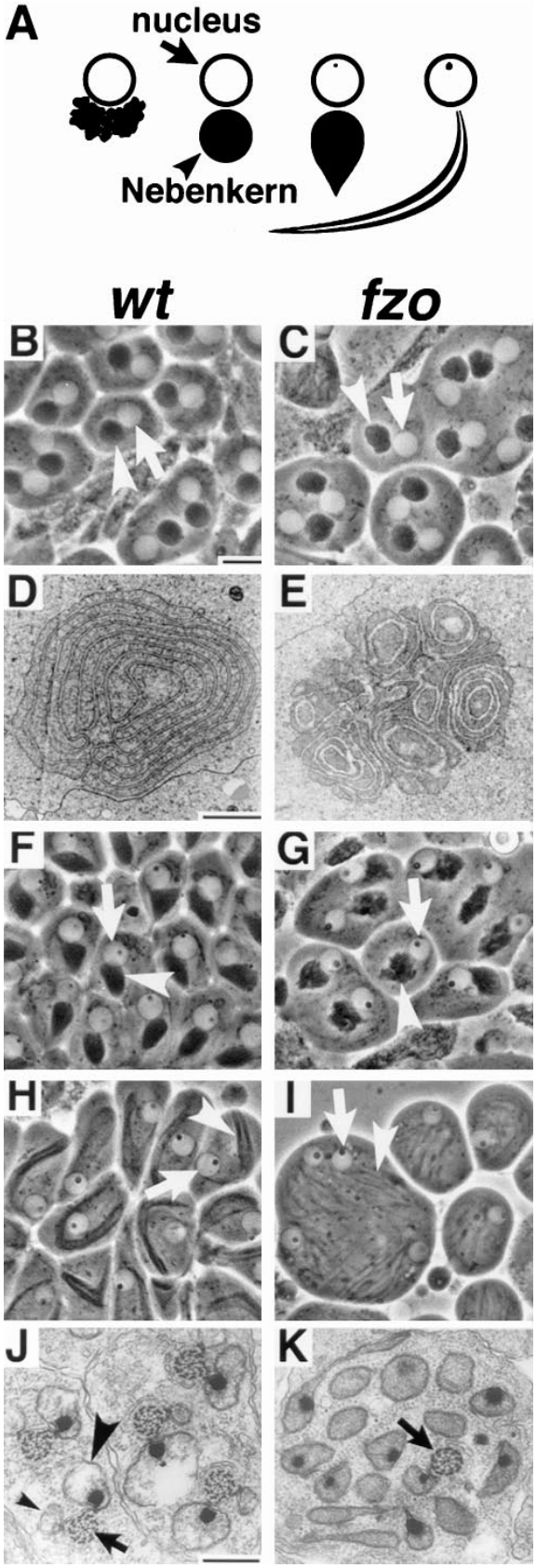

Figure 1. Mitochondrial Morphogenesis in Wild-Type and *fzo* Spermatids

(A) Diagram of wild-type mitochondrial morphogenesis. Nuclei, open; mitochondria, closed. Left to right: mitochondrial aggregation; onion stage; early elongation; mid-elongation. A protein body of unknown function appears in nuclei of elongating spermatids.

(B–K) Phase contrast (B, C, and F–I) and transmission electron (D, E, J, and K) micrographs of wild-type (B, D, F, H, and J) and *fzo*^{1} (C, E, G, I, and K) spermatids. Arrows indicate spermatid nuclei in (B), (C), and (F)–(I). Spermatids differentiate together in cysts of 64 cells; in (B), (C), and (F)–(I), some appear syncytial due to opening of cytoplasmic bridges between cells during sample preparation. (B and C) Onion stage spermatids with Nebenkerns (arrowheads) adjacent to nuclei. (D and E) Cross sections of onion stage Nebenkerns. Individual mitochondria in *fzo* (E) appear to wrap around each other, as do the two giant mitochondrial derivatives in wild type (D). (F and G) Early elongation stage spermatids with unfurling and elongating mitochondrial derivatives (arrowheads). Note the fragmented appearance of mitochondria in the mutant. (H and I) Mid-elongation stage spermatids with elongating mitochondrial derivatives (arrowheads). (J and K) Cross sections of elongating spermatids. In wild type (J), each axoneme (arrow) is associated with one major (large arrowhead) and one minor (small arrowhead) mitochondrial derivative. In the mutant (K), each axoneme (arrow) is associated with many mitochondrial derivatives, roughly half of which display dark paracrystalline material characteristic of major mitochondrial derivatives. Scale bars: 10 μm (B, C, and F–I); 2 μm (D and E); 0.5 μm (J and K).

Two ethylmethane sulfonate (EMS)–induced alleles, *fzo*^{1} and *fzo*^{2}, were characterized. *fzo*^{1}/*fzo*^{1}, *fzo*^{1}/*fzo*^{2}, *fzo*^{1}/*Df*(*3R*)*P2O*, and *fzo*^{2}/*Df*(*3R*)*P2O* flies showed identical phenotypes, suggesting that both mutations are strong loss-of-function alleles. The severity of the phenotype was consistent among all spermatids in all testes observed. The *fzo*^{1} and *fzo*^{2} mutations did not noticeably affect female fertility or overall viability.

fzo Encodes a Novel, Conserved, Predicted Transmembrane GTPase

The *fzo*^{1} mutation was mapped by recombination to an 11 kb genomic region using visible markers (Figure 2A) and restriction fragment length polymorphisms (RFLPs) (Figure 2B; see Experimental Procedures). A 12 kb deficiency [*Df*(*3R*)*P2O*] generated by imprecise excision of a nearby P element (*cnc*^{03871}) failed to complement *fzo* mutations, consistent with the RFLP mapping data (Figure 2B). cDNA clones corresponding to transcripts from the *fzo* region were isolated from a testis cDNA library, and all represented a single transcription unit; the largest cDNAs were 2.4 kb. A single copy of a 4 kb genomic fragment containing the candidate locus plus 1 kb upstream and approximately 500 bp downstream restored fertility and normal mitochondrial morphogenesis to *fzo* mutant males.

Sequence analysis of the *fzo* cDNA revealed a complete open reading frame (ORF) encoding a predicted protein of 718 amino acids (Figure 2C) with flanking AT-rich sequences and a single consensus translational start site (Cavener and Ray, 1991). Database searches identified related predicted proteins (see GenBank entries for references) in C. elegans (U29244, ORF 14, 28% identity), S. cerevisiae (Z36048, 19% identity), and mammals. Human expressed sequence tags (ESTs) homologous to *fzo* appear to derive from two different genes. We sequenced the cDNA clone from which a human fetal brain EST (T06373) was derived and showed that

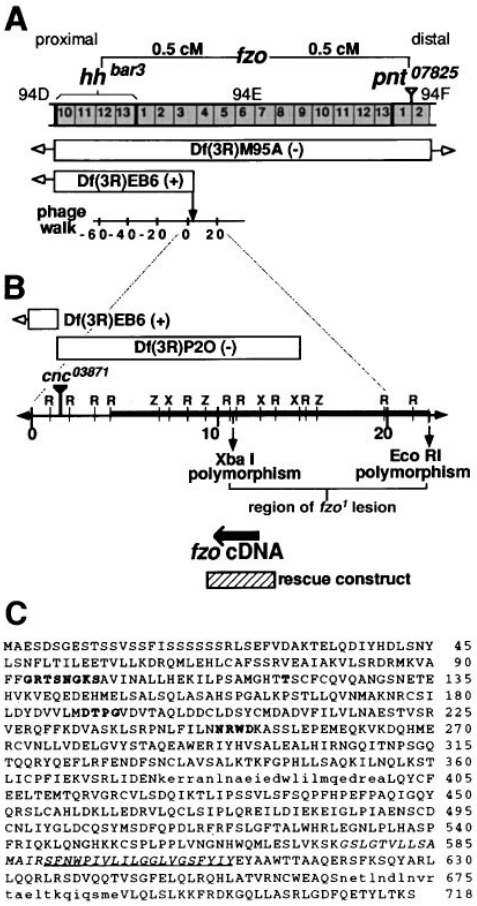

Figure 2. Molecular Cloning of *fzo*

(A) Genetic, cytological, and molecular map of the *fzo* region on chromosome 3R. Stippled, numbered boxes represent polytene chromosome bands; open bars are deficiencies, with (+) indicating complementation of *fzo* and (−) indicating failure to complement. The distal breakpoint of *Df(3R)EB6* is at +2 kb on a genomic phage walk (Mohler et al., 1991) that extends 90 kb distal from *hh*.

(B) Molecular map of the *fzo* region of the genomic walk, with coordinates 0–20 indicated in kb. Deficiencies are represented as in (A). Restriction sites: (R), EcoRI; (X), XbaI; and (Z), XhoI. Thick line on molecular map represents genomic DNA used to screen testis cDNA library.

(C) Predicted amino acid sequence (single letter amino acid code) of the *fzo* gene product, with regions matching GTPase motifs in boldface. Underlined region, predicted transmembrane domain (TMpred, Hofmann and Stoffel, 1993). Italics, large hydrophobic region including the predicted transmembrane domain and 13 adjacent uncharged residues (see Figure 3D). Lowercase, predicted coiled-coil regions with probability scores above 0.4 (Lupas et al., 1991; see Figure 3C).

it encodes an incomplete predicted protein with 35% identity to Fzo (Figure 3B). Heart (AA248162, AA248083), fibroblast (W49736), and other brain ESTs (R20140, T37724) are virtually identical to regions of this cDNA, while ESTs from liver/spleen (H58349) and pancreas (AA155601) seem to originate from a different gene and together encode a 125 residue peptide (not shown) 56% identical to the human brain gene product. Both human isoforms are 28% identical to Fzo in this C-terminal region. Four overlapping mouse ESTs (W41601,

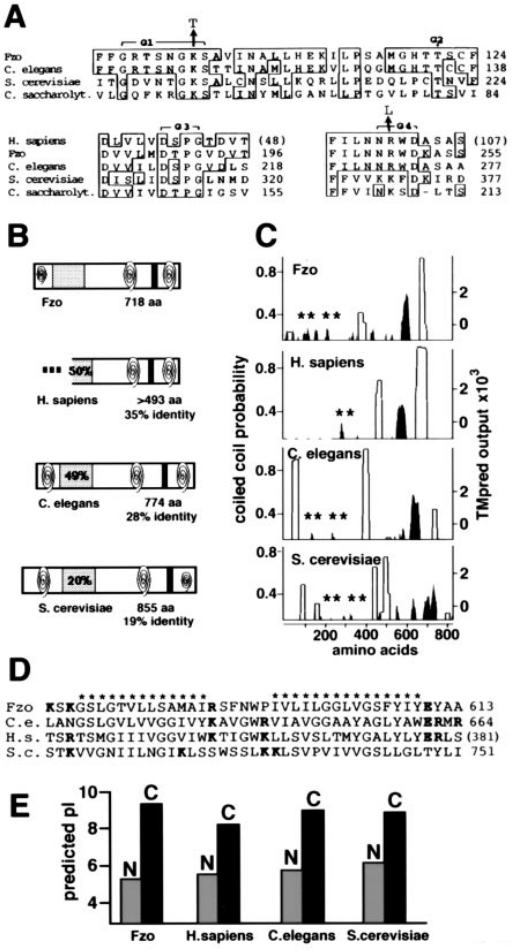

Figure 3. *fzo* Encodes a Conserved, Novel, Predicted Transmembrane GTPase

(A) Alignments of predicted GTPase motifs in Fzo and homologs, numbered G1–G4 as in Bourne et al. (1991). Boxes indicate identities with Fzo. The sequence of the H. sapiens homolog is unknown in the region of the G1 and G2 motifs. Introduced missense mutations are indicated by arrows above sequence alignment.

(B) Schematic diagram of Fzo and the H. sapiens fetal brain, C. elegans, and S. cerevisiae homologs, showing predicted GTPase domain (stippled box) and predicted transmembrane domain (closed bar). Spirals indicate predicted coiled-coil regions with probabilities between 0.4 and 1.0 (large spirals) and between 0.2 and 0.4 (small spirals) (see Experimental Procedures; the S. cerevisiae carboxy-terminal region has a higher coiled-coil probability [0.49] if window size 14 is used). Percentage identities to Fzo overall and within the predicted GTPase domains are indicated. Not shown are predicted C-terminal fragments of a different human homolog and a mouse homolog, as well as the C. saccharolyticum predicted amino-terminal protein fragment (see text).

(C) Overlaid plots of coiled-coil probabilities (open) and hydrophobicity (closed) as measured by TMpred; a TMpred output of 0.5 × 10^3 or above is considered significant (Hofmann and Stoffel, 1993). Stars represent GTPase motifs.

(D) Alignment of predicted transmembrane domain and surrounding region in Fzo and homologs. Charged residues are in boldface. Asterisks indicate conserved blocks of uncharged residues.

(E) Predicted isoelectric points for regions of Fzo and homologs after conceptual division at the transmembrane region. Shaded bars, amino terminus to transmembrane region; closed bars, transmembrane region to carboxyl terminus.

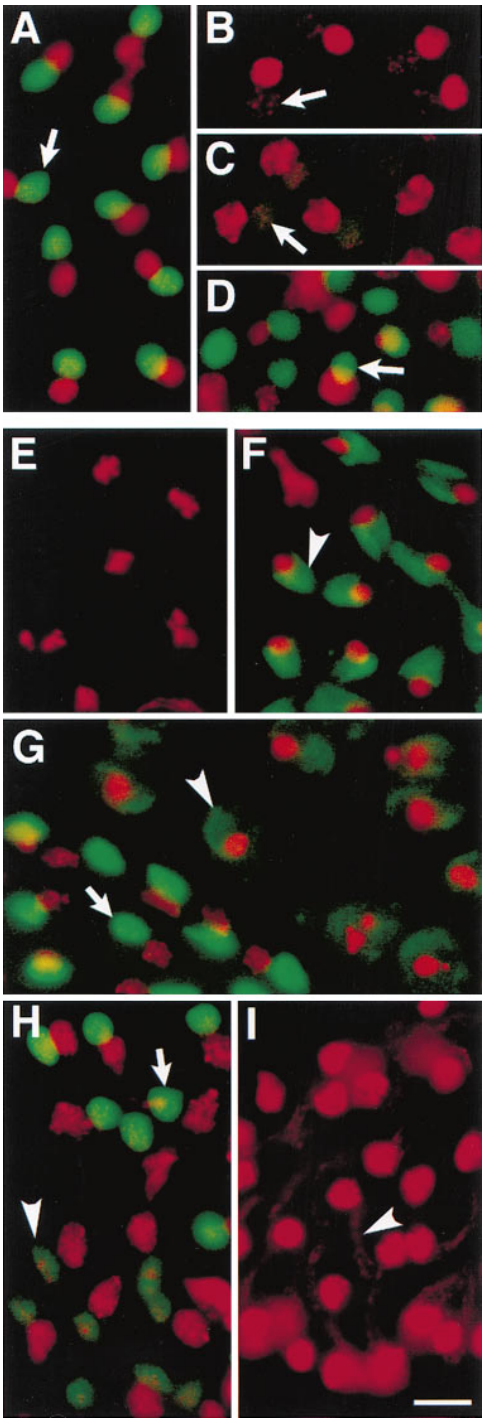

Figure 4. Fzo Is Associated with Mitochondria Only around the Time of Fusion

Indirect immunofluorescence images of cells stained with anti-Fzo$^{605–718}$ antiserum (green) and DAPI (red). (A–D) Onion stage spermatids as in Figure 1B (arrows, Nebenkerns). (A) wild type; (B) *fzo*^{1}/*fzo*^{1}; (C) *fzo*^{2}/*Df*(*3R*)*P2O*. Mitochondrial DNA visible in (B) and (C). (D) *fzo*^{1}/*fzo*^{1} flies carrying two copies of the *fzo*$^{+}$ transgene (D). (E–I) Wild-type cells from meiosis through spermatid elongation. (E) Metaphase I or II. (F) Telophase II. Fzo associated with mitochondria (arrowhead) on spindle remnant. (G) Cells from adjacent cysts showing relative Fzo levels on mitochondria at the aggregation (arrowhead) and onion (arrow) stages. (H) Cells from adjacent cysts showing relative Fzo levels on onion (arrow) and early elongation (arrowhead) stage Nebenkerns. (I) Mid-elongation stage spermatids (as in Figure 1H) with no detectable Fzo protein but visible mitochondrial DNA (arrowhead). Scale bar = 10 μm.

AA199015, AA212845, AA052806) together encode 211 amino acids with 22% identity to the Fzo carboxyl terminus and 84% identity to the analogous region from the human brain homolog (not shown). A predicted protein from the thermophilic bacterium C. saccharolyticum (L18965 ORF 6) is 11% identical to Fzo and 24% identical to the S. cerevisiae homolog.

The region of highest homology between Fzo and its human fetal brain, C. elegans, and S. cerevisiae homologs (50%, 49%, and 20% identity to Fzo, respectively) is a 186 amino acid region containing four completely conserved motifs found in virtually all GTPases (G1–G4 in Figure 3A; Bourne et al., 1991). The C. saccharolyticum predicted protein also contains these motifs (Figure 3A). Outside the individual motifs there is no significant similarity to any known GTPase. However, spacing between GTPase motifs, their N-terminal placement, and overall predicted protein size are reminiscent of the dynamin family (Warnock and Schmid, 1996). The G2 motif, a conserved threonine (Bourne et al., 1991), has not been defined in dynamins. Both the Fzo and dynamin families have a conserved threonine exactly 20 residues beyond the G1 motif that we propose represents G2 (Figure 3A).

Outside the GTPase domain, the human fetal brain, C. elegans, and S. cerevisiae homologs are 30%, 21%, and 19% identical to Fzo, respectively, and all share several predicted structural features. All have a predicted transmembrane domain near the carboxyl terminus (Figures 3B and 3C) embedded in a large (~34 amino acids) uncharged region interrupted by 1–3 basic residues (Figure 3D). The homologs have predicted coiled-coil regions flanking the predicted transmembrane domain (Figures 3B and 3C). All four homologs are acidic overall between the amino terminus and the transmembrane domain, with predicted isoelectric points (pI) near 5, and basic in the carboxy-terminal tail, with predicted pIs near 9 (Figure 3E).

Fzo Is Associated with Mitochondria during a Short Time Period Spanning Fusion

Antibodies raised against a fusion protein containing the C-terminal 115 residues of Fzo stained onion stage Nebenkerns brightly in wild-type spermatids (Figure 4A, arrow). Fzo was undetectable or present at greatly reduced levels in *fzo*^{1}/*fzo*^{1} or *fzo*^{2}/*Df*(*3R*)*P2O* testes, respectively (Figures 4B and 4C). A wild-type *fzo* transgene in a *fzo*^{1}/*fzo*^{1} mutant background restored detectable Fzo protein to the Nebenkern (Figure 4D).

The Fzo protein was associated with mitochondria in wild-type spermatids during a narrow developmental window corresponding to the time that Fzo function is required. Mitochondria align on the spindle equator throughout meiotic divisions (Fuller, 1993), but the Fzo protein was not detected on mitochondria until the last stages of meiosis II (Figures 4E and 4F). In postmeiotic haploid spermatids, Fzo was associated with aggregat-

ing mitochondria (Figure 4G, arrowhead) and was detected at highest levels on onion stage Nebenkerns (Figures 4G and 4H, arrows). Fzo was detected at lower levels associated with early elongation stage mitochondrial derivatives (Figure 4H, arrowhead) and was not detected on more elongated mitochondria (Figure 4I, arrow).

Conserved Residues in the GTPase Domain Are Required for Fzo Function but Not for Targeting of the Protein to Mitochondria

Mitochondrial fusion appears to require the predicted Fzo GTP-binding activity. Missense mutations that alter conserved residues (Figure 3A) required in other GTPases for guanine nucleotide binding (Sigal et al., 1986; Der et al., 1988; van der Bliek et al., 1993) were introduced into the *fzo* genomic rescue construct. Neither the fzo^{K99T} or fzo^{R249L} mutated transgene (in one or two copies) could restore fertility or sperm motility to *fzo* mutant males. The fzo^{K99T} transgene had no detectable effect on the subcellular mutant phenotype (Figure 5B), while the fzo^{R249L} transgene appeared to allow some mitochondrial fusion (Figure 5C). Neither mutant transgene showed a dominant effect in a wild-type background, even in multiple copies (not shown). The proteins encoded by the fzo^{K99T} and fzo^{R249L} mutated transgenes were properly localized to spermatid mitochondria (Figures 5D and 5E) with wild-type timing of appearance and disappearance (not shown).

Discussion

Fzo Is a Novel, Predicted GTPase

The Drosophila *fzo* gene encodes a predicted GTPase required for mitochondrial fusion during spermatogenesis and detected on mitochondria during a short time spanning the fusion event. Fzo contains four motifs common to virtually all known GTPases (Bourne et al., 1991) and conserved among Fzo homologs from mammals to yeast. Fzo is the first to be assigned a function in this new family of large, predicted transmembrane GTPases.

Mutations predicted to diminish guanine nucleotide binding did not affect localization of Fzo to mitochondria but eliminated or reduced its ability to mediate mitochondrial fusion. The fzo^{K99T} mutation, predicted to disallow key hydrogen bonds with the GTP β and γ phosphates (Pai et al., 1990; Noel et al., 1993), caused a severe loss of function phenotype (Figure 5B). In contrast, the fzo^{R249L} mutation appeared to allow some mitochondrial fusion to occur (Figure 5C), though not enough to restore normal sperm morphology or motility. The Fzo arginine 249 is part of the G4 motif and is predicted to contact the ribose moiety of GTP (Pai et al., 1990; Noel et al., 1993). Nearly all known GTPases have a lysine at positions analogous to Fzo^{R249} (Bourne et al., 1991); perhaps the conservative change to arginine in Fzo and its higher eukaryotic homologs reflects decreased importance of this residue for stable nucleotide binding. Mutations analogous to fzo^{R249L} in H-*ras* reduce but do not eliminate GTP binding (Der et al., 1988). Similarly, Fzo^{R249L} may have residual GTP affinity, allowing partial function.

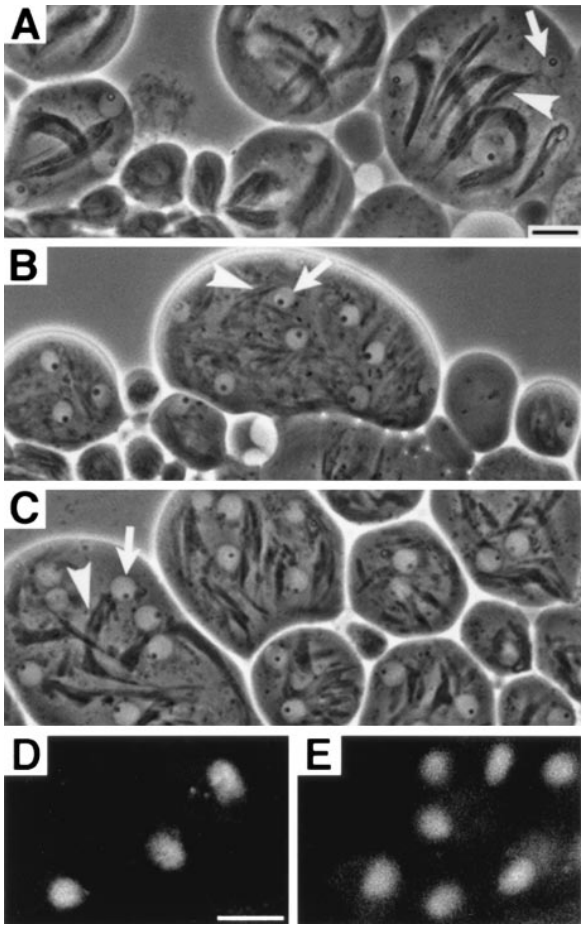

Figure 5. Mutations in the Predicted GTPase Domain Affect Fzo Function but Not Its Localization

(A–C) Mid-elongation stage spermatids from fzo^{1}/fzo^{1} males carrying two copies of a wild-type or mutated transgene. Compare with Figures 1H and 1I. Arrows, spermatid nuclei. Arrowheads, elongating mitochondrial derivatives. The fzo^{+} transgene (A) restored fertility and wild-type mitochondrial fusion, resulting in two elongating mitochondrial derivatives per spermatid. The fzo^{K99T} transgene (B) did not noticeably rescue the mutant phenotype. The fzo^{R249L} transgene (C) did not restore fertility but allowed some mitochondrial fusion to occur, resulting in fewer and larger mitochondrial derivatives (arrowhead) than in fzo^{1}/fzo^{1} but more than the normal two per spermatid.

(D and E) Immunofluorescence images of onion stage spermatids from fzo^{1}/fzo^{1} males carrying two copies of (D) the fzo^{K99T} transgene or (E) the fzo^{R249L} transgene, incubated with anti-$Fzo^{605–718}$ antiserum. Compare with the green channel from Figures 4B–4D. Mutated transgenes restore detectable protein to Nebenkerns in a fzo^{1}/fzo^{1} background. DNA staining (not shown) indicated nuclei adjacent to anti-Fzo-stained Nebenkerns, as in Figure 4A.

Scale bars = 10 μm for (A)–(C) and (D) and (E).

The fzo^{K99T} and fzo^{R249L} mutations are recessive. Analogous mutations in mammalian dynamins cause dominant-negative phenotypes when expressed in tissue culture cells (Herskovits et al., 1993; van der Bliek et al., 1993). Formation of macromolecular dynamin ring-shaped complexes appears to require GTP binding by all subunits (Warnock and Schmid, 1996). In contrast to dynamins, Fzo molecules may act individually or form complexes in which only some subunits must bind GTP for proper assembly or function.

Models for Fzo Orientation and Function

The conserved overall charge distribution and predicted transmembrane domain of the Fzo protein are consistent with a possible N_{out}-C_{in} orientation on mitochondria. Mitochondrial matrix proteins are typically more basic than cytoplasmic isoforms (Jaussi, 1995), and inner mitochondrial membrane proteins are generally basic in matrix-residing regions and more acidic in outside regions (Gavel and von Heijne, 1992). Fzo and homologs, when conceptually divided at their transmembrane domains, have amino termini with predicted pIs of 5.3–6 and carboxyl termini with pIs of 8.1–9.3 (Figure 3E), suggesting that the carboxyl terminus may reside in the mitochondrial matrix.

The Fzo protein has eight acidic residues and only one arginine in its first 50 amino acids, making import via a traditional amino-terminal targeting signal unlikely (von Heijne et al., 1989). Although the serine-rich nature of this region could allow mitochondrial targeting despite the acidic residues, Fzo may instead be targeted to mitochondria by an internal basic region just carboxy-terminal to the predicted transmembrane domain (e.g. residues 621–636), as is the S. cerevisiae Bcs1p protein (Fölsch et al., 1996).

The predicted transmembrane region of Fzo and homologs, which consists of two blocks of uncharged residues separated by a small region with one or more charged amino acids (Figure 3D), could potentially span a single membrane twice. Alternatively, as overall charge distribution in the protein suggests compartmental separation of the amino and carboxyl termini, it is plausible, although unprecedented, that Fzo could span both the inner and outer mitochondrial membranes at a contact site. With the C-terminal hydrophobic block in the inner membrane and the charged region in the intermembrane space, the N-terminal hydrophobic block could traverse the outer membrane in a β sheet conformation, which requires fewer hydrophobic residues to span the membrane than an α helix. This putative β sheet region could form lateral hydrogen bonds with other copies of itself or with β sheet transmembrane regions from other outer membrane proteins like porin (De Pinto and Palmieri, 1992). In mammalian tissue culture cells, mitochondrial fusion appears to initiate where inner/outer membrane contact sites on each of two separate mitochondria are apposed (Bereiter-Hahn and Voth, 1994). Stable inner/outer membrane contact sites that are independent of protein import channels have been observed (Glick and Schatz, 1991). Perhaps Fzo acts at such inner/outer membrane contact sites to mediate mitochondrial fusion.

If Fzo spans both membranes with its carboxyl terminus in the matrix, then the predicted GTPase domain and adjacent predicted coiled-coil regions would be oriented toward the cytoplasm. The Fzo protein could act as part of a ligand/receptor pair between separate mitochondria, binding to copies of itself or to other molecules displayed on the outer mitochondrial membrane. Alternatively, the Fzo protein could recruit other molecules to form a complex that links adjacent mitochondria. In either case, GTP binding and hydrolysis by Fzo may regulate the specificity of these interactions, as Rab GTPases seem to regulate formation of the SNARE complex prior to membrane fusion in the secretory and endocytic pathways (Pfeffer, 1996). Alternatively, the Fzo predicted GTPase may have a biomechanical role, as may dynamin GTPases in the formation of endocytic vesicles (Warnock and Schmid, 1996). GTP hydrolysis could cause a fusion-triggering conformational change in Fzo itself or in other recruited proteins, analogous to the mechanism by which hemagluttinin mediates bilayer mixing during fusion of influenza virus to cells (Hernandez et al., 1996). Future work will elucidate the mechanism by which Fzo acts.

Developmental Regulation of Fzo

The appearance of Fzo on spermatid mitochondria is developmentally regulated. Antibodies to the Fzo carboxyl terminus detected the protein on mitochondria only around the time of mitochondrial fusion, approximately four days after the initial appearance of *fzo* mRNA in primary spermatocytes (data not shown). Detection of Fzo was not simply a result of mitochondrial aggregation; mitochondria aggregate in early primary spermatocytes and align on the spindle during meiotic divisions (Fuller, 1993), but Fzo was first detected only after metaphase II. Expression of Fzo could be regulated at the translational level, as is typical of many gene products needed for postmeiotic spermatid differentiation (Schäfer et al., 1995). Alternatively, Fzo could be regulated posttranslationally to allow association with mitochondria or to unmask C-terminal epitopes. As mitochondria elongate, Fzo could be degraded or removed from mitochondrial membranes (becoming diffuse and undetectable), or C-terminal epitopes could be cleaved or masked.

The Fzo Family of Predicted GTPases

Fzo homologs could mediate mitochondrial fusion in other organisms and cell types. Spermatid mitochondria in the nematode X. theresiae (and likely in C. elegans) appear to undergo developmentally regulated fusion (Kruger, 1991), perhaps mediated by the nematode Fzo homolog. In the yeast S. cerevisiae, no mutants defective in mitochondrial fusion have been identified. We are currently analyzing whether the S. cerevisiae Fzo homolog plays a role in this process (G. Hermann, K. G. H., M. T. F., and J. Shaw, unpublished data). ESTs from genes encoding the human homologs were derived from brain, heart, pancreas, liver/spleen, and fibroblasts; mitochondrial fusion occurs in mammalian liver (Smith, 1931; Brandt et al., 1974) and may occur in neurons (Hayashida, 1973) and fibroblasts (Johnson et al., 1980). Mammalian spermatid mitochondria do not fuse but form structurally distinct contacts (Olson and Winfrey, 1992), which seem to allow connection between mitochondrial matrices (Zorov et al., 1990). Similar connections are also seen in rat cardiac tissue (Bakeeva et al., 1983) and may require protein mediators similar to those needed for full mitochondrial fusion in other cells. Analysis of possible roles of Fzo homologs in other organisms will allow assignment of a general function for this new family of large multidomain GTPases.

Experimental Procedures

Fly Strains and Culture

Flies were grown on standard media at 25°C. Visible markers and balancer chromosomes are described in FlyBase (FlyBase Consortium, 1996) unless otherwise noted. *Oregon R* was used as the wild-type strain. *Df(3R)M95A* (94D; 95A3) and *Df(3R)EB6* (94C2-5; 94E3) are described in Reuter et al. (1986) and Mohler et al. (1995). *Df(3R)P2O* was generated by mobilizing a ry^+-marked P element associated with the cnc^{03871} allele (Mohler et al., 1995) using the *Δ2–3* chromosomal source of transposase (Robertson et al., 1988). ry^- progeny were picked, and 200 independent mutagenized chromosomes were tested for failure to complement fzo^1. Molecular breakpoints of *Df(3R)P2O* were mapped by Southern blot analysis (Sambrook et al., 1989). *Df(3R)P2O* failed to complement mutations in *cnc* and was therefore not homozygous viable.

fzo^1 was isolated in a screen for EMS-induced recessive male sterile mutations by J. Hackstein (1991). fzo^2 was isolated in a screen of 1799 EMS-treated third chromosomes, as described in Lin et al. (1996), except that mutagenized chromosomes were tested for failure to complement fzo^1. Fertility and viability tests of the allelic combinations fzo^1/fzo^1, fzo^1/fzo^2, $fzo^1/Df(3R)P2O$, and $fzo^2/Df(3R)P2O$ were as in Lin et al., (1996). The fzo^2 chromosome carried a secondary lethal.

Light and Electron Microscopy

Light microscopy of live squashed testis preparations was as in Lin et al. (1996). To assess mitochondrial membrane potential, 10 μg/ml rhodamine 123 (Johnson et al., 1980) was included in the dissection buffer and samples examined under epifluorescence.

Testes were prepared for TEM as in Tokuyasu (1974), except that 1% paraformaldehyde was included in the fixative, samples were stained for 1 hr in 1% uranyl acetate before ethanol dehydration, and testes were embedded in Spurr's resin. Thin sections (80–90 nm) were examined on a Phillips 410 transmission electron microscope.

Recombination Mapping

fzo^1 was initially mapped to roughly 9 cM distal of *e* by analyzing single recombinants between an *e* fzo^1 chromosome and a *ru h th st* p^p *cu sr ca* chromosome. fzo^1 was more finely mapped to 0.58 ± 0.17 cM distal of hh^{bar3} based on 227 progeny (recombinant between *hh* and *tx*) from p^p *e* fzo^1/hh^{bar3} *tx* females.

The fzo^1 mutation was further localized with respect to RFLPs between hh^{bar3} and a ry^+-marked P element insertion associated with the pnt^{07825} allele. Briefly, recombinants between ry^{506} hh^{bar3} fzo^1 parental chromosome 1) and ry^{506} P(ry^+)pnt^{07825} (parental chromosome 2) were scored for inheritance of the fzo^1 mutation. Recombinants either hh^{bar3-} ry^- or hh^{bar3+} ry^- appeared at a frequency of 31 in 2995 flies, placing hh^{bar3} and P(ry^+)pnt^{07825} 1.04 ± 0.18 cM apart. The fzo^1 mutation mapped in the center of the interval, 0.5 cM distal to hh^{bar3} and 0.5 cM proximal to P(ry^+)pnt^{07825} (Figure 2A). RFLPs between the two parental chromosomes were identified by Southern blot analysis of genomic DNA from flies homozygous for parental chromosome 1 as well as from flies transheterozygous for parental chromosomes 1 and 2. DNAs were digested separately with 34 standard four-, five-, and six-cutter restriction enzymes and probed with fragments from the distal third of a 90 kb genomic walk in the region (Mohler et al., 1991; Figure 2). Segregation of RFLPs was then scored in 35 recombinants. Analysis of linkage between the RFLPs and fzo^1 placed the fzo^1 mutation between a polymorphic XbaI site at +11 and a polymorphic EcoRI site at +22 on the genomic walk. The XbaI and EcoRI RFLPs were separated from fzo^1 in one and two of the 35 recombinants, respectively.

Isolation of cDNAs and Sequence Analysis

A λZAP (Stratagene) testis cDNA library (T. Hazelrigg) was probed with cloned DNA fragments corresponding to +5–+22 on the genomic walk (Mohler et al., 1991; Figure 2B), yielding 18 positive cDNA clones, which all derived from the same transcription unit based on Southern blot hybridization. The seven longest cDNAs had 2.4 kb inserts and identical restriction maps; one was mapped to genomic DNA by Southern blot hybridization and sequenced fully on both strands by dideoxy chain termination (Sanger, 1977) using T3 or T7 primers on the cDNA or dropout subclones and 19- or 20-mer oligonucleotides (PAN facility, Stanford) to fill remaining gaps. Representative shorter cDNAs were restriction mapped, partially sequenced, and shown to be truncated versions of the longer cDNA.

The Fzo predicted protein sequence was used to search nucleotide sequence databases translated in all reading frames (BLAST; Altschul et al., 1990). The cDNA clone from which a human fetal brain EST (GenBank T06373) was derived was obtained from American Type Culture Collection and sequenced on one strand. Alignments were done with the help of the CLUSTALW program (Thompson et al., 1994) using DNAstar. Structural features were analyzed using TMpredict (Hofmann and Stoffel, 1993), COILS (MDITK matrix, weighted second and fifth heptad positions, window size 21; Lupas et al., 1991), and Compute pI/Mw (ExPASy Molecular Biology Server).

P Element–Mediated Germline Transformation and Construction of Mutated Transgenes

A 3 kb XhoI/XbaI DNA fragment corresponding to +9–+12 on the genomic walk (Figure 2B) was subcloned into the w^+-marked P element transformation vector pCaSpeR4 (Thummel and Pirrotta, 1992) to make plasmid pKH2. A 1 kb XbaI/EcoRI fragment corresponding to +11–+12 on the walk was subcloned into pKH2 to make pKH3fzo$^+$. The resulting 4 kb insert in the pKH3fzo$^+$ rescue construct contained the genomic region of the 2.4 kb *fzo* cDNA plus approximately 1 kb 5′ and 500 base pairs 3′.

pKH3fzo$^+$ was introduced into *y* w^{67} or w^{1118} flies by P element–mediated germline transformation (Rubin and Spradling, 1982). Four independent fzo^+ insertions, two on the second chromosome and two on the third, were isolated and crossed into *w; fzo* mutant backgrounds by independent assortment or recombination.

To introduce mutations into the Fzo predicted GTP-binding domain, a 1.8 kb XbaI/BamHI restriction fragment representing the first two thirds of the *fzo* coding region from pKH3fzo$^+$ was subcloned into Bluescript SK(−). Oligomutagenesis (Sambrook et al., 1989), was performed separately with 5′-ACCTCAAATGGAACTAGTG CCGTGATC-3′ and 5′-TACTCAACAATCTATGGGATAAG-3′. The former exchanged AA for CT at nucleotide positions 369–370 in the *fzo* cDNA, introducing a SpeI restriction site and changing lysine 99 to threonine. The latter replaced G with T at nucleotide 819, eliminating a ClaI restriction site and changing arginine 249 to leucine. Mutagenized constructs were selected by altered restriction sites. For each mutagenized construct, a 1.8 kb XbaI/BamHI restriction fragment was ligated with the 10 kb XbaI/BamHI fragment from plasmid pKH3fzo$^+$ to create pKH3fzo^{K99T} and pKH3fzo^{R249L}. In both cases, the XbaI and BamHI restriction sites used for the final subcloning were regenerated by the ligations, and the reading frame remained unchanged at the mutagenesis and subcloning sites, as shown by detection of mutant proteins with C-terminal-specific antibodies.

Flies were transformed with the fzo^{K99T} and fzo^{R249L} mutant transgenes as above, yielding eight and five independent second chromosome transgene insertions, respectively, all of which were separately introduced into *fzo* mutant backgrounds by independent assortment. To test for dominant effects, males with one wild-type copy of *fzo* and as many as four (fzo^{K99T}) or six (fzo^{R249L}) different copies of the mutated transgenes were generated by appropriate crosses.

Generation of Anti-Fzo$^{604–718}$ Antibodies

To make an expression construct encoding a fusion protein with a 6-histidine tag and the C-terminal 115 amino acids of Fzo, the 0.5 kb BamHI/HindIII restriction fragment from the *fzo* cDNA (HindIII site from Bluescript SK[−]) was subcloned into pQE30 (QIAGEN). The fusion protein was expressed in bacteria and purified on a Ni-NTA column with imidazole elution (QIAexpressionist, QIAGEN). The purest fractions were dialyzed in 1.5 M urea, 0.1 M Na phosphate, 0.01 M Tris–HCl, and 500 mM NaCl (pH 7). The fusion protein precipitated at urea concentrations below 4 M. After dialysis, precipitated protein was emulsified in complete Freund's adjuvant and injected into rabbits using standard schedules for initial (500 mg) and booster (250 mg) injections and for serum collections (Berkeley Antibody Company, Richmond, CA).

Immunofluorescence

Testes were prepared for immunofluorescence staining as in Hime et al. (1996). Slides were incubated overnight at 4°C in preimmune or anti-Fzo$^{604–718}$ serum diluted 1:150 in PBTB (phosphate-buffered saline with 0.1% Triton X-100 and 3% bovine serum albumin), washed four times at room temperature in PBTB, and incubated for one hour at 37°C in FITC-conjugated anti-rabbit IgG (Jackson Labs) diluted 1:200 in PBTB. Slides were washed 4 × 10 minutes in PBTB, with 1 μg/ml DAPI in the second wash, and mounted in 85% glycerol, 2.5% N-propyl gallate. Samples were examined using epifluorescence on a Zeiss Axiophot microscope and images collected with a Photometrics cooled CCD camera (courtesy of B. Baker). Emissions from different fluorochromes on the same sample were collected separately and overlaid using Adobe Photoshop.

Acknowledgments

Correspondence regarding this paper should be addressed to M. T. F. (e-mail: fuller@cmgm.stanford.edu). We thank J. Hackstein for *fzo*^{1}, J. Mohler for genomic clones, and G. Reuter for *Df(3R)M95A*. P element insertions near *fzo* were obtained from the Bloomington Drosophila Stock Center. For TEM assistance, we thank F. Thomas; for helping with mutagenesis screens, we acknowledge P. Ibara, J. Kim, J. Lee, A. Lehman, D. Rixter, S. Sun, and J. William. We thank T. Hazelrigg for the testis cDNA library, M. Fish for assistance in making transgenic flies, and B. Baker for use of the CCD camera. The Stanford PAN facility generated oligonucleotides and helped with DNA sequencing. Special thanks to J. Brill for copious general advice, D. Clayton for helpful comments throughout this work, and R. Scheller, G. Shadel, and the Fuller lab for critical reading of the manuscript. This work was supported by National Institutes of Health (NIH) grant 1RO1-HD29194 to M. T. F., and by both a predoctoral fellowship from the Howard Hughes Medical Institute and an NIH training grant, HG00044yr2 for 1996–97, to K. G. H.

Received April 2, 1997; revised May 27, 1997.

References

Altschul, S.F., Gish, W., Miller, W., Myers, E.W., and Lipman, D.J. (1990). Basic local alignment search tool. J. Mol. Biol. *215*, 403–410.

Bakeeva, L.E., Chentsov, Y.S., and Skulachev, V.P. (1983). Intermitochondrial contacts in myocardiocytes. J. Mol. Cell. Cardiol. *15*, 413–420.

Bakeeva, L.E., Chentsov, Y.S., and Skulachev, V.P. (1981). Ontogenesis of mitochondrial reticulum in rat diaphragm muscle. Eur. J. Cell. Biol. *25*, 175–181.

Bereiter-Hahn, J., and Voth, M. (1994). Dynamics of mitochondria in living cells: shape changes, dislocations, fusion, and fission of mitochondria. Microsc. Res. Tech. *27*, 198–219.

Bourne, H.R., Sanders, D.A., and McCormick, F. (1991). The GTPase superfamily: conserved structure and molecular mechanism. Nature *349*, 117–127.

Brandt, J.T., Martin, A.P., Lucas, F.V., and Vorbeck, M.L. (1974). The structure of rat liver mitochondria: a reevaluation. Biochem. Biophys. Res. Comm. *59*, 1097–1103.

Cavener, D.R., and Ray, S.C. (1991). Eukaryotic start and stop translation sites. Nucleic Acids Res. *19*, 3185–3192.

De Pinto, V.D., and Palmieri, F. (1992). Transmembrane arrangement of mitochondrial porin or voltage dependent anion channel (VDAC). J. Bioenerg. Biomembr. *24*, 21–26.

Der, C.J., Weissman, B., and MacDonald, M.J. (1988). Altered guanine nucleotide binding and H-*ras* transforming and differentiating activities. Oncogene *3*, 105–112.

Dujon, B. (1981). Mitochondrial genetics and functions. In The Molecular Biology of the Yeast Saccharomyces: Life Cycle and Inheritance, J.N. Strathern, E.W. Jones, and J.R. Broach, eds. (Cold Spring Harbor, NY: Cold Spring Harbor Press), pp. 505–635.

FlyBase Consortium. (1996). FlyBase: the Drosophila database. Nucleic Acids Res. *24*, 53–56.

Fölsch, H., Guiard, B., Neupert, W., and Stuart, R.A. (1996). Internal targeting signal of the BCS1 protein: a novel mechanism of import into mitochondria. EMBO J. *15*, 479–487.

Fuller, M.T. (1993). Spermatogenesis. In The Development of Drosophila, M. Bate and A. Martinez-Arias, eds. (Cold Spring Harbor, New York: Cold Spring Harbor Press), pp. 71–147.

Gavel, Y., and von Heijne, G. (1992). The distribution of charged amino acids in mitochondrial inner-membrane proteins suggests different modes of membrane integration for nuclearly and mitochondrially encoded proteins. Eur. J. Biochem. *205*, 1207–1215.

Glick, B., and Schatz, G. (1991). Import of proteins into mitochondria. Annu. Rev. Genet. *25*, 21–44.

Hackstein, J.H.P. (1991). Spermatogenesis in Drosophila. A genetic approach to cellular and subcellular differentiation. Eur. J. Cell Biol. *56*, 151–169.

Hayashida, Y. (1973). Gigantic mitochondria of spinal ganglion cells in rat. Cytobiologie *7*, 289–296.

Hernandez, L.D., Hoffman, L.R., Wolfsberg, T.G., and White, J.M. (1996). Virus-cell and cell-cell fusion. Annu. Rev. Cell Dev. Biol. *12*, 627–661.

Herskovits, J.S., Burgess, C.C., Obar, R.A., and Vallee, R.B. (1993). Effects of mutant rat dynamin on endocytosis. J. Cell Biol. *122*, 565–578.

Hime, G.R., Brill, J., and Fuller, M.T. (1996). Assembly of ring canals in the male germ line from structural components of the contractile ring. J. Cell Sci. *109*, 2779–2788.

Hofmann, K., and Stoffel, W. (1993). TMbase—a database of membrane spanning protein segments. Biol. Chem. Hoppe Seyler *347*, 166.

Jaussi, R. (1995). Homologous nuclear-encoded mitochondrial and cytosolic isoproteins. Eur. J. Biochem. *228*, 551–561.

Johnson, L.V., Walsh, M.L., and Chen, L.B. (1980). Localization of mitochondria in living cells with rhodamine 123. Proc. Natl. Acad. Sci. USA *77*, 990–994.

Kawano, S., Takano, H., and Kuroiwa, T. (1995). Sexuality of mitochondria: fusion, recombination, and plasmids. Int. Rev. Cytol. *161*, 49–110.

Kirkwood, S.P., Munn, E.A., and Brooks, G.A. (1986). Mitochondrial reticulum in limb skeletal muscle. Am. J. Physiol. *251*, C395–C402.

Kruger, J.C.D.W. (1991). Ultrastructure of sperm development in the plant-parasitic nematode Xiphinema theresiae. J. Morphol. *210*, 163–174.

Lin, T.-Y., Viswanathan, S., Wood, C., Wilson, P.G., Wolf, N., and Fuller, M.T. (1996). Coordinate developmental control of the meiotic cell cycle and spermatid differentiation in Drosophila males. Development *122*, 1331–1341.

Lupas, A., Van, D.M., and Stock, J. (1991). Predicting coiled coils from protein sequences. Science *252*, 1162–1164.

Mayer, A., Wickner, W., and Haas, A. (1996). Sec18p (NSF)-driven release of Sec17p (α-SNAP) can precede docking and fusion of yeast vacuoles. Cell *85*, 83–94.

Mohler, J., Mahaffey, J.W., Deutsch, E., and Vani, K. (1995). Control of Drosophila head segment identity by the bZIP homeotic gene *cnc*. Development *121*, 237–247.

Mohler, J., Vani, K., Leung, S., and Epstein, A. (1991). Segmentally restricted, cephalic expression of a leucine zipper gene during Drosophila embryogenesis. Mech. Dev. *34*, 3–10.

Noel, J.P., Hamm, H.E., and Sigler, P.B. (1993). The 2.2 Å crystal structure of transducin-α complexed with GTPγS. Nature *366*, 654–663.

Olson, G.E., and Winfrey, V.P. (1992). Structural organization of surface domains of sperm mitochondria. Mol. Reprod. Dev. *33*, 89–98.

Pai, E.F., Krengel, U., Petsko, G.A., Goody, R.S., Kabsch, W., and Wittinghofer, A. (1990). Refined crystal structure of the triphosphate conformation of H-ras p21 at 1.35 Å resolution: implications for the mechanism of GTP hydrolysis. EMBO J. *9*, 2351–2359.

Pfeffer, S.R. (1996). Transport vesicle docking: SNAREs and associates. Annu. Rev. Cell Dev. Biol. *12*, 441–461.

Rancourt, M.W., McKee, A.P., and Pollack, W. (1975). Mitochondrial profile of a mammalian lymphocyte. J. Ultrastruct. Res. *51*, 418–424.

Reuter, G., Dorn, R., Wustmann, G., Freide, B., and Rauh G. (1986). Third chromosome suppressor of position-effect variegation loci in *Drosophila melanogaster*. Mol. Gen. Genet. *202*, 481–487.

Robertson, H., Preston, C., Phillis, R., Johnson-Schlitz, D., Benz, W., and Engels, W. (1988). A stable genomic source of P element transposase in Drosophila melanogaster. Genetics *188*, 461–470.

Rothman, J.E. (1996). Protein machinery of vesicle budding and fusion. Prot. Sci. *5*, 185–194.

Rubin, G.M., and Spradling, A.C. (1982). Genetic transformation of Drosophila with transposable element vectors. Science *218*, 348–353.

Sambrook, J., Fritsch, E.F., and Maniatis, T. (1989). Molecular Cloning: A Laboratory Manual (Cold Spring Harbor, NY: Cold Spring Harbor Laboratory Press).

Sanger, F., Nicklen, S., and Coulsen, A.R. (1977). DNA sequencing with chain-terminating inhibitors. Proc. Natl. Acad. Sci. USA *74*, 5463–5467.

Schäfer, M., Nayernia, K., Engel, W., and Schäfer, U. (1995). Translational control in spermatogenesis. Dev. Biol. *172*, 344–352.

Sigal, I.S., Gibbs, J.B., D'Alonzo, J.S., Temeles, G.L., Wolanski, B.S., Socher, S.H., and Scolnick, E.M. (1986). Mutant ras-encoded proteins with altered nucleotide binding exert dominant biological effects. Proc. Natl. Acad. Sci. USA *83*, 952–956.

Skulachev, V.P. (1990). Power transmission along biological membranes. J. Membr. Biol. *114*, 97–112.

Smith, D.M. (1931). The ontogenic history of the mitochondria of the hepatic cell of the white rat. J. Morphol. Physiol. *52*, 485–512.

Stevens, B. (1981). Mitochondrial structure. In The Molecular Biology of the Yeast Saccharomyces: Life Cycle and Inheritance, J.N. Strathern, E.W. Jones, and J.R. Broach, eds. (Cold Spring Harbor, NY: Cold Spring Harbor Press), pp. 471–504.

Takano, H., Kawano, S., and Kuroiwa, T. (1994). Genetic organization of a linear mitochondrial plasmid (mF) that promotes mitochondrial fusion in *Physarum polycephalum*. Curr. Genet. *26*, 506–511.

Tates, A.D. (1971). Cytodifferentiation during spermatogenesis in Drosophila melanogaster: an electron microscope study (Leiden: Rijksuniversiteit).

Thompson, J.D., Higgins, D.G., and Gibson, T.J. (1994). CLUSTAL W: improving the sensitivity of progressive multiple alignment through sequence weighting, position-specific gap penalties and weight matrix choice. Nucleic Acids Res. *22*, 4673–4680.

Thummel, C.S., and Pirrotta, V. (1992). Technical notes: new pCasper P-element vectors. Dros. Inf. Serv. *71*, 150.

Tokuyasu, K.T. (1974). Dynamics of spermiogenesis in *Drosophila melanogaster*. III. Relation between axoneme and mitochondrial derivatives. Exp. Cell. Res. *84*, 239–250.

van der Bliek, A., Redelmeir, T.E., Damke, H., Tisdale, E.J., Meyerowitz, E.M., and Schmid, S.L. (1993). Mutations in human dynamin block an intermediate stage in coated vesicle formation. J. Cell. Biol. *122*, 553–563.

von Heijne, G., Steppuhn, J., and Herrmann, R.G. (1989). Domain structure of mitochondrial and chloroplast targeting peptides. Eur. J. Biochem. *180*, 535–545.

Warnock, D.E., and Schmid, S.L. (1996). Dynamin GTPase, a force-generating molecular switch. BioEssays *18*, 885–893.

Zorov, D.B., Skulachev, V.P., and Khalangk, V. (1990). Membranous electric cable: 4. Mitochondrial helix of rat spermatazoan. Biol. Membr. *7*, 243–249.

GenBank Accession Numbers

The GenBank accession numbers for the *fzo* cDNA and for the partial cDNA encoding the *fzo* human fetal brain homolog are U95821 and U95822, respectively.